

## Identification of *Ether à Go-Go* and Calcium-Activated Potassium Channels in Human Melanoma Cells

R. Meyer<sup>1</sup>, R. Schönherr<sup>1</sup>, O. Gavrilova-Ruch<sup>1</sup>, W. Wohlrab<sup>2</sup>, S.H. Heinemann<sup>1</sup>

<sup>1</sup>Arbeitsgruppe Molekulare und zelluläre Biophysik am Klinikum der Friedrich-Schiller-Universität Jena, Drackendorfer Strasse 1, D-07747 Jena, Germany

<sup>2</sup>Martin-Luther-Universität Halle, Medizinische Fakultät, Dermatologische Klinik, Ernst-Kromayer-Str. 5/6, D-06097 Halle, Germany

Received: 5 February 1999/Revised: 28 May 1999

**Abstract.** Ion channels and intracellular  $\text{Ca}^{2+}$  are thought to be involved in cell proliferation and may play a role in tumor development. We therefore characterized  $\text{Ca}^{2+}$ -regulated potassium channels in the human melanoma cell lines IGR1, IPC298, and IGR39 using electrophysiological and molecular biological methods. All cell lines expressed outwardly rectifying  $\text{K}^+$  channels. Rapidly activating delayed rectifier channels were detected in IGR39 cells. The activation kinetics of voltage-gated  $\text{K}^+$  channels in IGR1 and IPC298 cells displayed characteristics of *ether à go-go* (eag) channels as they were much slower and depended both on the holding potential and on extracellular  $\text{Mg}^{2+}$ . In addition, they could be blocked by physiological concentrations of intracellular  $\text{Ca}^{2+}$ . In accordance with these electrophysiological results, analysis of mRNA revealed the expression of a gene coding for h-eag1 channels in IGR1 and IPC298 cells, but not in IGR39 cells. At elevated  $\text{Ca}^{2+}$  concentrations various types of  $\text{Ca}^{2+}$ -activated  $\text{K}^+$  channels with single-channel characteristics similar to IK and SK channels were detected in IGR1 cells. The whole-cell  $\text{Ca}^{2+}$ -activated  $\text{K}^+$  currents were not voltage dependent, insensitive for 100 nM apamin and 200  $\mu\text{M}$  *d*-tubocurarine, but were blocked by charybdotoxin (100 nM) and clotrimazole (50 nM). Analysis of mRNA revealed the expression of hSK1, hSK2, and hIK channels in IGR1 cells.

**Key words:** Potassium channel — Melanoma — *Ether à go-go* channel — Intracellular  $\text{Ca}^{2+}$  — Proliferation — Patch clamp

## Introduction

Melanoma is a rapidly proliferating and highly metastatic tumor, which responds poorly to chemo- and radiotherapy. Therefore, other methods are necessary for an efficient and specific inhibition of the progression of this form of cancer. Ion channels, and especially potassium ( $\text{K}^+$ ) channels, are thought to be involved in tumor progression and thus may be targets for new anti-tumor drugs. First attempts using  $\text{K}^+$  channel blockers (i.e., tetraethylammonium (TEA), 4-aminopyridine (4-AP), quinidine) revealed new ways to influence proliferation of tumor cells, i.e., neuroblastoma, lymphoma, or breast cancer cells (reviewed in Wonderlin & Strobl, 1996). In addition, the proliferation of melanoma cell lines (IGR1, SK MEL 28) could be influenced by relatively unspecific  $\text{K}^+$  channel blockers (TEA, quinidine), which induced membrane depolarization (Nilius & Wohlrab, 1992; Lepple-Wienhues et al., 1996). Membrane depolarization induced by elevated extracellular  $\text{K}^+$  concentrations inhibited proliferation of cycling cells in a similar way (Lepple-Wienhues et al., 1996; Wonderlin & Strobl, 1996). These studies provide some evidence that membrane hyperpolarization, or at least a lack of depolarization, is necessary for the progression of the cell cycle. A possible mechanism for transforming membrane potential changes to intracellular signals, which mediate the cellular response, may be a coupling to the intracellular  $\text{Ca}^{2+}$  concentration ( $[\text{Ca}^{2+}]_i$ ). Hyperpolarization of the membrane by activation of  $\text{K}^+$  channels could provide or maintain a sufficiently large driving force for  $\text{Ca}^{2+}$  entry (Nilius, Schwarz & Droogmans, 1993). In this way elevated  $[\text{Ca}^{2+}]_i$  levels, necessary for cell-cycle progression, can be obtained.

In this study we characterized  $\text{K}^+$  channels in the

human melanoma cell line IGR1, which was established from a metastatic tumor in groin lymph node. In addition, we tested IGR39 and IPC298 cells, which have been established from primary cutaneous tumors. Studying these cells, we concentrated on  $K^+$  channels, which are linked to the intracellular  $Ca^{2+}$  concentration. The most obvious candidates are those  $K^+$  channels that are activated by intracellular  $Ca^{2+}$ . These  $K(Ca^{2+})$  channels are often characterized by their single-channel conductance, terming them BK (large conductance), IK (intermediate conductance), and SK (small conductance)  $Ca^{2+}$ -activated channels. IK and SK channels are voltage-independent and activate at relatively low  $[Ca^{2+}]_i$ , while BK channels are activated at higher  $[Ca^{2+}]_i$  and display some voltage dependence, yielding a higher open probability at positive voltages (for a review see Vergara et al., 1998). We use here the term IK for intermediate conductance channels, but it should be noted that the corresponding gene has been cloned independently by different groups (Joiner et al., 1997; Ishi et al., 1997b; Logsdon et al., 1997) resulting in different names: SK4, IK, and KCa4.

More recently, outwardly rectifying voltage-activated  $K^+$  channels, which are inhibited by low  $[Ca^{2+}]_i$ , have been characterized. The channels belong to the *ether à go-go* family of genes and are therefore termed eag channels. The variants cloned from rat (Ludwig et al., 1994) and human (Occhiodoro et al., 1998) are both half-inhibited by about 100 nM  $[Ca^{2+}]_i$  (Stansfeld et al., 1996; Bijlenga et al., 1998). These channels have been functionally characterized in human neuroblastoma cells (Meyer & Heinemann, 1998). Interestingly, in this cell line h-eag channels are only expressed in nondifferentiated cells indicating a very tight coupling of h-eag expression to the cell cycle (Meyer & Heinemann, 1998). In human myoblasts, h-eag channels also appear to play a critical role in early stages of the cells as they are responsible for the hyperpolarization-induced cell fusion (Bijlenga et al., 1998). Thus, both IK/SK and eag potassium channels are potential candidates of  $K^+$  channels, which respond to modest excursions from the basal level of intracellular  $Ca^{2+}$  and which may provide a coupling to the cell cycle.

Using both electrophysiological and molecular biological methods, we could identify h-eag1 channels in IGR1 and IPC298 cells.  $K(Ca^{2+})$  channels were investigated in IGR1 cells revealing the expression of hSK1, hSK2, and hIK isoforms. Both channel types, h-eag and hIK/hSK are regulated by intracellular  $Ca^{2+}$ , although in opposite directions, and are therefore putative elements of cellular feedback mechanisms in melanoma cells.

## Materials and Methods

### CELL CULTURE

Melanoma cell lines IGR1, IPC298, and IGR39 (German Collection of Microorganisms and Cell Cultures, Department of Human and Animal

Cell Cultures, Braunschweig, Germany) were routinely cultured in Dulbecco's modified Eagle's medium containing 10% fetal calf serum, and incubated at 37°C in a humidified atmosphere with 10%  $CO_2$ . For electrophysiological recordings cells were trypsinized and plated in petri dishes or glass-bottom petri dishes, if experiments involving fluorescence measurements had to be performed. The recordings started about 1–2 days after plating.

### ELECTROPHYSIOLOGY

Experiments were performed at room temperature in the whole-cell or inside-out patch-clamp configuration, using an EPC9 (HEKA Elektronik, Lambrecht, Germany) patch-clamp amplifier. Pulse protocol generation as well as data acquisition was controlled with the program Pulse (HEKA Elektronik). Data from whole-cell patch-clamp experiments were corrected routinely for leak currents and capacitive transients using a P/n method. Series resistance errors were compensated in the range of 50–80%. When using aspartate solutions, the pipette potential was corrected for a liquid junction potential of +11 mV. Patch pipettes were fabricated from Kimax-51 glass (Kimble Glass, Vineland, NJ) with resistance values in the range of 1–5 M $\Omega$ .

The programs PulseFit (HEKA Elektronik) and Igor-Pro (WaveMetrics, Lake Oswego, OR) were used for data analysis. The rise time of h-eag channel activation ( $t_r$ ) as a function of the prepulse voltage (V) was described by a first-order Boltzmann function (Fig. 2b):

$$t_r(V) = t_r(\infty) + \frac{t_r(-\infty) - t_r(\infty)}{1 + \exp(-(V - V_{1/2})/k)} \quad (1)$$

where  $V_{1/2}$  denotes the midpoint of this distribution and  $k$  is a measure for the steepness.

The standard extracellular solution was composed of (mM): 5 KCl, 135 NaCl, 2  $MgCl_2$ , 2  $CaCl_2$ , and 10 Hepes (pH 7.4). Solutions with various  $Mg^{2+}$  concentrations were mixed from extracellular solutions containing no or 10 mM  $Mg^{2+}$ . In some cases the extracellular solution was supplemented with 5 mM glucose. The standard intracellular solution with no free calcium was (mM): 130 KAsp, 10 NaCl, 2  $MgCl_2$ , 10 EGTA, and 10 Hepes (pH 7.4). An intracellular solution with about 0.8  $\mu M$  free calcium was made by addition of 9.3 mM  $CaCl_2$  to the standard intracellular solution. Extracellular solutions were changed by total exchange of the entire bath volume or by using an application system that was placed directly in front of the cell or the patch, respectively.

### MEASUREMENT OF INTRACELLULAR FREE $Ca^{2+}$

Changes of intracellular free calcium concentration ( $[Ca^{2+}]_i$ ) were detected fluorimetrically using the dye Fura-2 (100  $\mu M$ ), loaded via the patch pipette. Fluorescence measurements were performed with a combination of a scanning monochromator and a photomultiplier (Polychrome I, TILL Photonics, Planegg, Germany), mounted to an inverted microscope (Axiovert 100, Carl Zeiss, Jena, Germany) with a 40 $\times$  objective (Neofluar, Carl Zeiss). Data acquisition was performed with the X-Chart extension of Pulse (HEKA Elektronik). Fluorescence values were corrected for background fluorescence recorded before loading the cells with Fura-2. Cells were illuminated at 355 nm and 385 nm for 50 msec, and the ratio ( $R$ ) of the emitted light intensities was used to calculate the free intracellular calcium concentration according to (Neher, 1995):

$$[Ca^{2+}]_i = K_{eff} \frac{R - R_{min}}{R_{max} - R} \quad (2)$$

The calibration constants  $R_{max}$  and  $R_{min}$  were obtained in separate experiments with no ( $R_{min}$ ) and 10 mM intracellular calcium ( $R_{max}$ ). The effective dissociation constant  $K_{eff}$  was calculated according to:

$$K_{eff} = K_D \frac{R_{max} + \alpha}{\alpha + R_{min}} \quad (3)$$

The dissociation constant of Fura-2 ( $K_D$ ) of 220 nM was used and the isocoefficient  $\alpha$  was determined empirically (0.1).

Ionomycin (5  $\mu$ M) was applied to the cells to increase the intracellular calcium concentration. The dose-response curve for the block of h-eag channel activity by intracellular calcium was described by a Hill function (Fig. 4b):

$$I = \frac{I_{max}}{1 + ([Ca^{2+}]_i / IC_{50})^n} \quad (4)$$

$I_{max}$  denotes the maximal current,  $IC_{50}$  the calcium concentration of half-maximal block, and  $n$  the Hill coefficient.

## MOLECULAR BIOLOGY

Messenger RNA (mRNA) from IGR1, IPC298, and IGR39 cells was isolated with the OligoTex Direct mRNA Kit (Qiagen, Hilden, Germany) and mRNA from approximately  $5 \times 10^4$  cells was used for each RT-PCR (reverse transcriptase polymerase chain reaction). RT-PCR was performed with the Titan OneTube RT-PCR Kit (Boehringer Mannheim GmbH, Mannheim, Germany) on a T3 Thermocycler (Biometra, Göttingen, Germany). Gene-specific primers were designed based on published human sequences for h-eag1 (AJ001366), hSK1 (U69883), hSK2 (EST AA418096), hSK3 (AF031815), hIK (AF022150), and hBK (U23767). The numbers given in parentheses are GenBank accession numbers. The primers for hSK2 were based on the EST sequence AA418096, which had been identified through a BLAST search for human homologues to the rat SK2 protein. This EST potentially encodes the last 72 amino acid residues of hSK2 with 70 identities to rSK2. The following primers (MWG-Biotech, Ebersberg, Germany) were used: h-eag1 sense-primer: 5'-TCC TCG TTG TAT TTC ACA ATG ACC-3', h-eag1 antisense-primer: 5'-ATG GGC AAG GGT GGT TTC C-3' (nt. 1273-1887), hSK1 sense-primer: 5'-CTA CTG CAC AGC AAA ATC TTC ACG-3', hSK1 antisense-primer: 5'-CCT GGT ATG TTT GTA GAT GAG CCA C-3' (nt. 790-1284), hSK2 sense-primer: 5'-GGA AAC AAA ACT AGA GAC TTT GAT TGG-3', hSK2 antisense-primer: 5'-TCT CTG ATG AAG TTG GTG GTG C-3' (nt. 9-211 of EST AA418096), hSK3 sense-primer: 5'-GCA TCT CTC TGT GGA TCA TTG C-3', hSK3 antisense-primer: 5'-AAT CTG CTT CTC CAG GTC TTC G-3' (nt. 144-1968), hIK sense-primer: 5'-TCA ATC AAG TCC GCT TCC G-3', hIK antisense-primer: 5'-ATT CTG CTG CAG GTC ATA CAG G-3' (nt. 554-1152), hBK sense-primer: 5'-GCA TCT CTC TGT GGA TCA TTG C-3', hBK antisense-primer: 5'-AAT CTG CTT CTC CAG GTC TTC G-3' (nt. 472-1355). The nucleotide numbers in parentheses correspond to the coding regions of the tested genes and identify the fragments predicted to be amplified by the primer pairs.  $\beta$ -actin primers included in the RT-PCR kit were used for control reactions, testing the function of the PCR reaction. The RT-PCR protocol was: incubation at 50°C for 30 min, 94°C for 60 sec, followed by 32 cycles of 94°C for 40 sec, 55°C for 30 sec, 72°C for 90 sec (prolonged by 1 sec per cycle) and a final incubation at 72°C for 7 min. 20  $\mu$ l aliquots of the reactions (50  $\mu$ l total) were run on 2%-agarose gels and the product size was estimated by comparison with a DNA standard (1 kb DNA ladder; Life Tech-

nologies GmbH, Eggenstein, Germany). The PCR products of h-eag1, hSK1, hSK2, and hIK were isolated from the gel with a Qiaquick Gel Extraction Kit (Qiagen), then cloned into the pGEM-T vector (Promega, Madison, WI), and finally sequenced.

All chemicals were obtained from Sigma except for Fura-2 (Calbiochem, San Diego, CA).

## Results

### VOLTAGE-DEPENDENT ACTIVATION OF $K^+$ CHANNELS IN VARIOUS HUMAN MELANOMA CELL LINES

When assayed with whole-cell patch-clamp recordings, most cells of the human melanoma cell lines IGR1 and IPC298 revealed slowly activating, outwardly rectifying  $K^+$  channels. These channels showed no inactivation and seemed to be the only voltage-activated  $K^+$  channels in these cells. In 163 IGR1 cells tested we only found a few without outwardly rectifying  $K^+$  channels as shown in Fig. 1a; the mean current at +50 mV carried by these channels was  $600 \pm 40$  pA (max. 2.4 nA). In two out of 163 cells currents mediated by rapidly activating delayed rectifier channels were measured. Slowly activating channels were also detected in 12 out of 17 tested IPC298 cells; the other cells had no or only very small outward  $K^+$  currents. In 7 out of 12 tested IGR39 cells, another human melanoma cell line, rapidly activating  $K^+$  channels were observed, which inactivated slowly during prolonged membrane depolarization (*not shown*); in the remaining cells no or only very small  $K^+$  currents were found.

The activation kinetics of both kinds of  $K^+$  channels, i.e., slowly and rapidly activating channels, were differentially influenced by the holding voltage. The activation of the  $K^+$  channels expressed in IGR1 and IPC298 cells became considerably slower after clamping the cells for 10 sec to -130 mV than after holding them at -60 mV (Fig. 1a and b). The holding voltage, however, did not influence activation kinetics of  $K^+$  channels in IGR39 cells (Fig. 1c).

The  $K^+$  channels in the three cell lines tested are voltage-gated outward rectifiers with threshold activation potentials in the range of -20 to -50 mV (Fig. 1, right). The voltage dependence, activation kinetics, and the degree of inactivation after long depolarizations suggest that the  $K^+$  channels expressed in IGR1 and IPC298 cells belong to the eag  $K^+$  channel family, while IGR39 cells expressed delayed rectifier channels.

### DETECTION OF mRNA SPECIFIC FOR H-EAG1 IN IGR1 AND IPC298 CELLS

To test for the expression of eag genes in melanoma cell lines we isolated mRNA and performed RT-PCR analysis for eag-specific mRNA. In accordance with the electrophysiological results, DNA fragments with the ex-

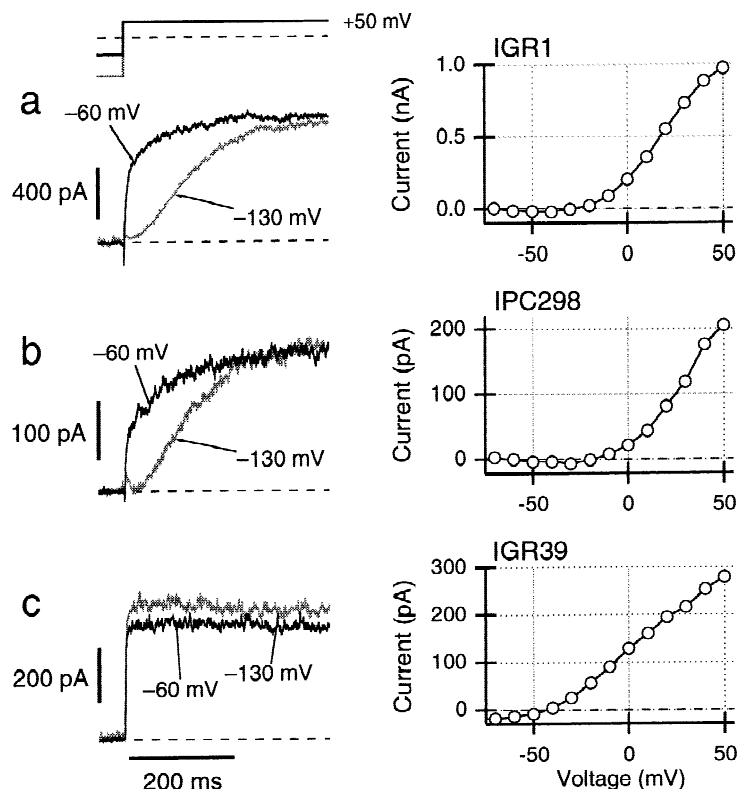


**Fig. 1.** Discrimination of  $K^+$  channels by their dependence on the holding membrane potential. Electrophysiological data were obtained from the melanoma cell lines IGR1 (a), IPC298 (b), and IGR39 (c). The left panels show current traces recorded in the whole-cell patch-clamp mode with the indicated voltage protocol. The cells were clamped for 10 sec to two different holding voltages ( $-130$  and  $-60$  mV) and then depolarized ( $+50$  mV) to activate  $K^+$  channels. After holding at  $-130$  mV, the activation of  $K^+$  channels in IGR1 (a) and IPC298 (b) cells was slower than after holding at  $-60$  mV. A pronounced dependence of the activation kinetics on the holding voltage is typical for eag channels. In contrast, the activation kinetics of the  $K^+$  channels in IGR39 (c) cells was independent of the holding voltage. The right panels show typical current-voltage curves of the three investigated melanoma cell lines. The plotted current values were determined at the end of 400-msec depolarizations to the indicated values.

pected length were obtained from IGR1 and IPC298 cells (Fig. 2a lane 4 and Fig. 2b lane 3, respectively). No product could be amplified from mRNA isolated from IGR39 (Fig. 2b lane 5). Residual genomic DNA was excluded as a source for the PCR reaction by control reactions without reverse transcription (Fig. 2a lane 2 and Fig. 2b lane 2) or after digesting mRNA with RNase (Fig. 2a lane 3). The efficiency of the RT-PCR reaction was tested with specific primers for  $\beta$ -actin (Fig. 2b lane 1+4). The sequence of the DNA fragment amplified from IGR1 and IPC298 cells was identical to that of h-eag1, recently cloned from human myoblasts (Occhiodoro et al., 1998). We therefore conclude that h-eag1 channels, like those expressed in human myoblasts, are expressed in IGR1 and IPC298 cells. However, we can not exclude deviations of the melanoma eag channels in those parts of the sequence, which are not covered by the analyzed fragment.

#### HOLDING POTENTIAL AND EXTRACELLULAR $Mg^{2+}$ INFLUENCE EAG CHANNELS OF IGR1 CELLS

A similar influence of the holding voltage on the activation kinetics as found for the  $K^+$  channels of IGR1 and IPC298 cells (Fig. 1a and b) was described for cloned eag channels from rat (Ludwig et al., 1994) and bovine (Frings et al., 1998) and was also observed for h-eag

channels expressed in human neuroblastoma cells (Meyer & Heinemann, 1998). In addition, the voltage dependence of the activation kinetics of these eag channels was modified by extracellular divalent ions (Terlau et al., 1996; Frings et al., 1998; Meyer & Heinemann, 1998). Therefore, we tested the influence of varying extracellular  $Mg^{2+}$  concentrations on the activation kinetics of  $K^+$  channels expressed in IGR1 cells. Current traces recorded from one IGR1 cell at varying extracellular  $Mg^{2+}$  concentrations are shown in Fig. 3a. Each family of superimposed current traces are responses to consecutive pulses to  $+50$  mV where the holding voltage (10 sec before each depolarization) was varied between  $-130$  and  $-40$  mV in steps of 10 mV. This protocol allows a more exact investigation of the influence of the holding voltage on the activation kinetics of  $K^+$  channels. Hyperpolarized holding voltages ( $-130$  mV) resulted in a slower activation than more positive holding voltages ( $-40$  mV). Increasing extracellular  $Mg^{2+}$  concentrations made this effect more clear and additionally slowed the activation of  $K^+$  channels. In particular, very negative holding voltages produce clearly sigmoidal activation time courses. The time to reach 80% of the maximum current was measured and plotted vs. the holding potential (Fig. 3b). The prepulse dependence of the risetime marks a transition from slowly activating to rapidly activating channel states (Fig. 3b). Increasing extracellular  $Mg^{2+}$  concentration shifted this transition to more positive voltages. The transition was characterized by a first-



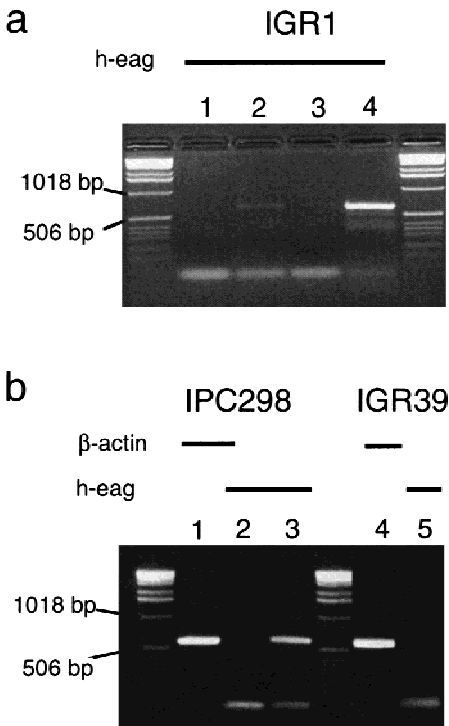


**Fig. 2.** Expression of mRNA coding for h-eag1 channels in melanoma cell lines. (a) Agarose gel with RT-PCR products obtained with specific primers for h-eag1 from IGR1 mRNA. Lane 1: no mRNA was used as negative control. Lane 2: the reaction was performed without reverse transcription to exclude DNA as source for the PCR reaction. The dim band is probably the result of incomplete inactivation of the reverse transcriptase (1 min 94°C) before the start of the PCR. Lane 3: the mRNA was first degraded with RNase before the RT-PCR reaction was started. This excludes DNA as source of the PCR-reaction. Lane 4: the band with the expected length of 615 bp shows that h-eag1 channels are expressed in IGR1 cells. (b) Agarose gel with PCR products obtained from IPC298 (lanes 1 to 3) and IGR39 cells (lanes 4 and 5). In lane 1 and 4, specific primers for  $\beta$ -actin were used to test for the efficiency of the RT-PCR reaction yielding positive signals (587 bp) in both cell lines. Lane 2: PCR was performed without reverse transcription. Lane 3: the expected band (615 bp) indicates the presence of mRNA coding for h-eag1 in IPC298 cells. Lane 5: in IGR39 cells no mRNA coding for h-eag1 was detected.

order Boltzmann function (Eq. 1) and the resulting mid-potentials ( $V_{1/2}$ ) are listed in the legend to Fig. 3. In 5 mM extracellular  $Mg^{2+}$   $V_{1/2}$  was  $-68 \pm 4$  mV and the slope factor  $11.7 \pm 1.6$  mV ( $n = 8$ ). These functional properties are very similar to those found for cloned rat and bovine eag channels expressed in *Xenopus* oocytes (Terlau et al., 1996; Schönherr et al., 1999) and h-eag channels in human neuroblastoma cells (Meyer & Heine-mann, 1998).

#### VOLTAGE-GATED $K^+$ CHANNELS IN IGR1 CELLS ARE BLOCKED BY INTRACELLULAR $Ca^{2+}$

As r-eag channels are blocked by low concentrations of intracellular  $Ca^{2+}$  (Stansfeld et al., 1996), we also tested the  $K^+$  channels of IGR1 cells for this property. Simul-

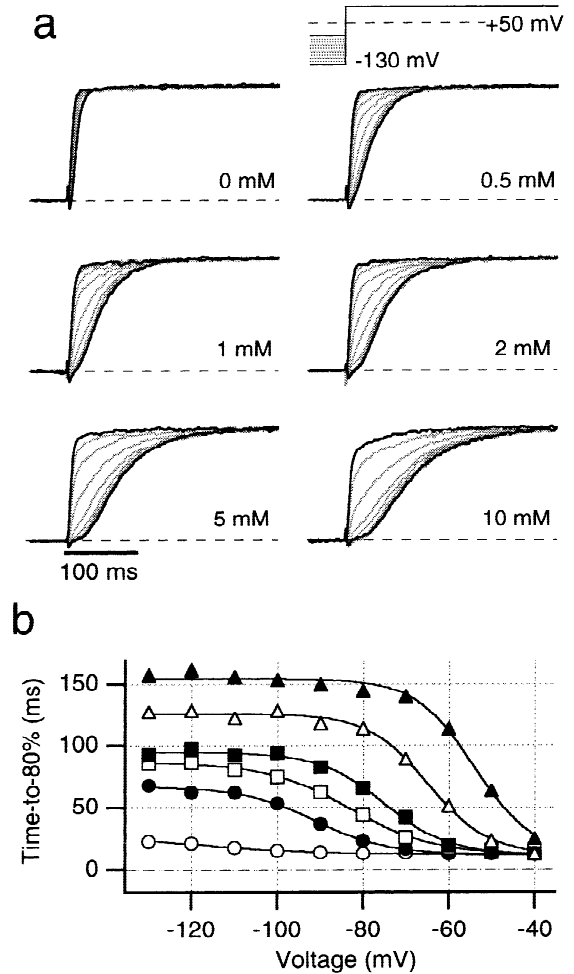


**Fig. 3.** Outwardly rectifying  $K^+$  channels in IGR1 cells show characteristics typical for h-eag channels. (a) Current traces were recorded from an IGR1 cell in the whole-cell patch-clamp configuration, filtered at 500 Hz. The cell was clamped for 10 sec to varying holding voltages ( $-130$  to  $-40$  mV) before the  $K^+$  channels were activated by membrane depolarization to  $+50$  mV. Holding at very hyperpolarized voltages ( $-130$  mV) resulted in slower activation kinetics than holding at more positive voltages. The experiment was performed with different  $[Mg^{2+}]_o$ , as indicated. Increasing  $[Mg^{2+}]_o$  slowed the activation kinetics of the  $K^+$  channels. The pronounced dependence of the activation kinetics on the holding voltage as well as the effect of  $Mg^{2+}_o$  is characteristic for eag channels. For clarity current traces obtained from  $-130$  and  $-40$  mV holding voltage are shown in black, the others in gray. (b) From the current traces shown in (a) the time to reach 80% of maximal current was obtained and plotted vs. the holding voltage. A transition from slow to fast activation is observed. This transition is shifted to more positive voltage by increasing  $[Mg^{2+}]_o$ . The curves indicated fits to Boltzmann functions (Eq. 1), which yielded the following half-maximal voltages,  $V_{1/2}$ : no  $Mg^{2+}$ ,  $-120.8$  mV (open circles); 0.5 mM  $Mg^{2+}$ ,  $-91.2$  mV (filled circles); 1 mM  $Mg^{2+}$ ,  $-83.0$  mV (open squares); 2 mM  $Mg^{2+}$ ,  $-75.1$  mV (filled squares); 5 mM  $Mg^{2+}$ ,  $-64.8$  mV (open triangles); 10 mM  $Mg^{2+}$ ,  $-54.1$  mV (filled triangles).

taneous recordings of current and  $Ca^{2+}$  concentration were performed in the whole-cell configuration; cells were loaded with the  $Ca^{2+}$ -sensitive dye Fura-2 (100  $\mu$ M) via the patch pipette. The outwardly rectifying  $K^+$  cur-

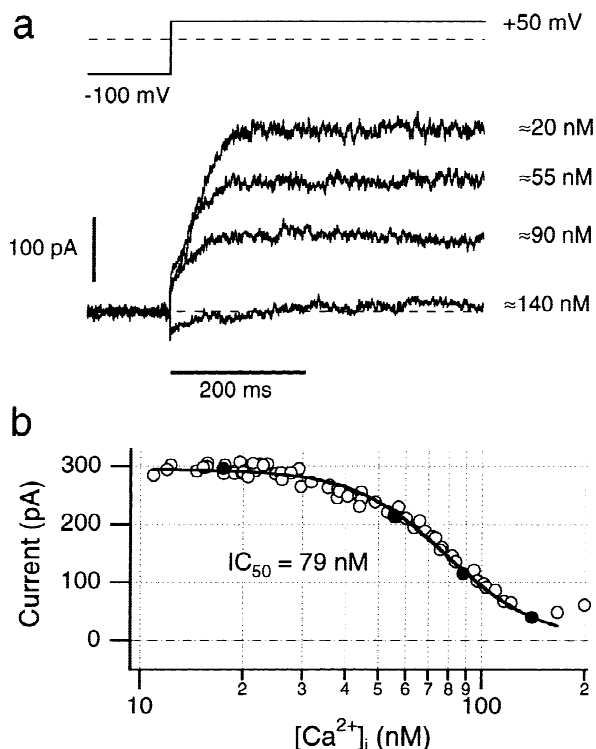


**Fig. 4.** Eag channels in IGR1 cells are blocked by intracellular  $Ca^{2+}$ . The intracellular  $Ca^{2+}$  concentration was measured fluorimetrically. In parallel,  $K^+$  currents were recorded in the whole-cell configuration. Depolarizations to +50 mV were applied every 5 sec; the holding voltage was -100 mV.  $[Ca^{2+}]_i$  was increased by application of 5  $\mu$ M ionomycin to the cell. (a) Selected current traces recorded before and during application of ionomycin. Ionomycin-induced elevation of  $[Ca^{2+}]_i$  blocked the voltage-gated  $K^+$  channels of IGR1 cells.  $[Ca^{2+}]_i$  values are indicated for the individual current traces. (b) Mean currents recorded at the end of the depolarizing pulses were plotted vs. the measured  $Ca^{2+}$  concentration. The indicated  $IC_{50}$  value was determined by fitting the Hill equation (Eq. 4) to the data points. The filled circles mark the data points obtained from the current traces shown in a. Data points above 150 nM  $Ca^{2+}$  were not considered for the fit.

rent of IGR1 cells was inhibited by application of the  $Ca^{2+}$  ionophore ionomycin (5  $\mu$ M), which induced an increase of the intracellular  $Ca^{2+}$  concentration (Fig. 4a). From the dose-response curves (Fig. 4b) an  $IC_{50}$ -value of  $99 \pm 29$  nM and a Hill coefficient of  $3.3 \pm 0.2$  ( $n = 2$ ) was obtained by fitting Eq. 4 to the data. These values are very close to those found for recombinant r-eag channels (Stansfeld et al., 1996) and indicate that  $K^+$  channels of IGR1 belong to the eag family. Since the  $IC_{50}$ -value is near to the basal  $Ca^{2+}$  concentration, this channel is sensitive to changes in  $[Ca^{2+}]_i$  in the physiological range.

#### EXPRESSION OF $Ca^{2+}$ -ACTIVATED POTASSIUM CHANNELS

Data shown in Fig. 4b already indicate an increase in outward current at +50 mV when the intracellular  $Ca^{2+}$

concentration rises above about 150 nM. At these  $[Ca^{2+}]_i$  values, current at -100 mV also increases indicating a  $Ca^{2+}$ -activated conductance with little voltage dependence. In inside-out patches from IGR1 cells an increase of the  $Ca^{2+}$  concentration from zero to about 0.8  $\mu$ M opened channels passing outward current at +50 mV. Linear voltage ramps revealed no voltage dependence of these channels and a reversal potential of about -80 mV, which is near to the theoretical reversal potential for  $K^+$  of -82.3 mV in the used physiological solutions (*not shown*). A single-channel conductance of  $7.8 \pm 2.3$  pS ( $n = 8$ ) was obtained from linear fits to current-voltage relationships. In symmetrical high  $K^+$  solutions, however, single-channel events of inhomogeneous sizes, ranging from small to intermediate conductance, were observed. The presence of many different channel types complicated a clear-cut electrophysiological characterization on the single-channel level. Nevertheless, these channel properties, i.e., the lack of voltage dependence, activation at submicromolar  $[Ca^{2+}]_i$ , and the conductance ranging from a few pS to about 50 pS are indicative of  $Ca^{2+}$ -activated  $K^+$  channels of the SK (small-conductance) or IK (intermediate-conductance) type.

To characterize the total contribution of  $K(Ca^{2+})$  channels in IGR1 cells, we measured currents in the whole-cell configuration as responses to linear voltage ramps from -100 to +50 mV. With 0.8  $\mu$ M free internal  $Ca^{2+}$  the ramp current-voltage relationships were almost linear with the expected reversal potential for  $K^+$  (Fig. 5). In 16 cells tested, this protocol yielded an average current at +50 mV of  $1.8 \pm 0.3$  nA (range 0.2–4.5 nA). Application of 100 nM charybdotoxin (ChTx), which is known to be a blocker for BK channels (large-conductance  $Ca^{2+}$ -activated  $K^+$  channels), IK channels (Ishi et al., 1997b), and some voltage-gated  $K^+$  channels, reduced the current by  $68 \pm 5\%$  ( $n = 3$ ). Apamin at 100 nM ( $n = 3$ ) and *d*-tubocurarine at 200  $\mu$ M concentration ( $n = 4$ ) did not block these currents. 50 nM clotrimazole, however, reduced the current by  $55 \pm 6\%$  ( $n = 6$ ). Thus, the  $K(Ca^{2+})$  channels in melanoma cells are apamin and *d*-tubocurarine insensitive, but sensitive to ChTx and clotrimazole. The sensitivity towards ChTx and apamin is similar to the channels studied by Peña & Rane (1997), which are hypothesized to be involved in growth factor regulation of both cell proliferation and differentiation.

To address the question, which individual  $Ca^{2+}$ -activated  $K^+$  channels are expressed in IGR1 cells, we performed RT-PCR analysis for the expression of different  $Ca^{2+}$ -activated  $K^+$  channels with mRNA isolated from this cell line. Specific primer pairs were used to test hSK1, hSK2, hSK3, hIK, and hBK mRNA. Fragments of the expected sizes were obtained for hSK1 (495 bp), hSK2 (203 bp) and hIK (599 bp) (Fig. 6a), but no products were obtained if the reverse transcription was

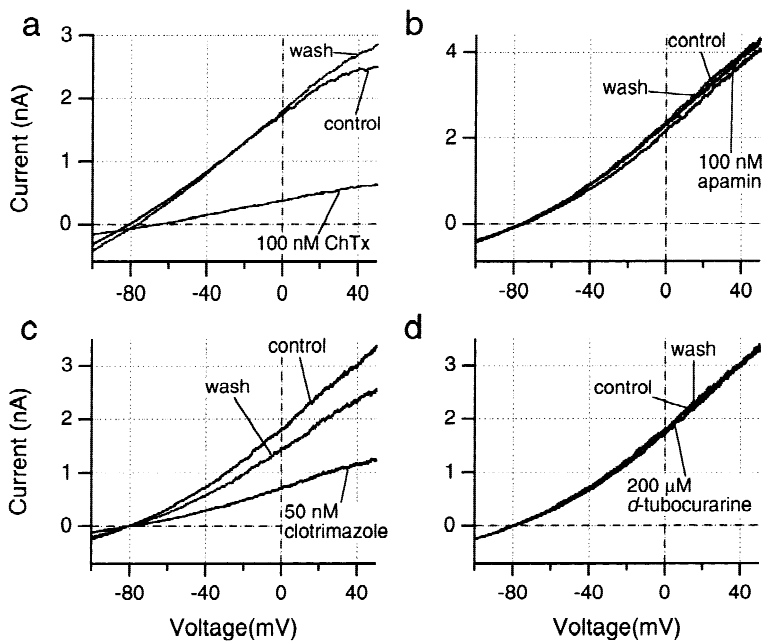


**Fig. 5.** Pharmacology of  $K(Ca^{2+})$  channels in IGR1 cells. The effect of various blockers on  $Ca^{2+}$ -activated  $K^+$  channels in IGR1 cells was tested in the whole-cell configuration with  $0.8 \mu M$  free  $Ca^{2+}$  in the pipette solution. Currents were measured as responses to voltage ramps (from  $-100$  to  $+50$  mV). (a)  $100$  nM ChTx reversibly blocked the currents in this case by about  $80\%$ . Note that the reversal potential is close to  $-80$  mV in the control and wash traces, indicating only small contributions of non-specific leak currents. Upon block by ChTx, the relative contribution of leak currents is increased, thus shifting the reversal potential to the positive direction (here about  $10$ – $15$  mV). (b) Application of  $100$  nM apamin; (c)  $50$  nM clotrimazole; (d)  $200 \mu M$   $\alpha$ -tubocurarine.

omitted, excluding the possibility of contaminating genomic DNA as template for the PCR products (Fig. 6b). No specific bands corresponding to the predicted products could be observed using primers for hSK3 and hBK (data not shown), indicating that these channels are not expressed in IGR1 cells. The amplified products of hSK1, hSK2, and hIK were further analyzed by DNA sequencing. All three fragments were completely identical to the corresponding parts of published sequences deposited in GenBank.

## Discussion

The investigation of functional properties of melanoma cells is an important precondition for the development of strategies for anti-tumor therapeutics. Therefore, various human melanoma cell lines have been studied in the past using electrophysiological methods. A large variety of different types of ionic currents have been measured in, e.g., C8161, C8146, C832C, and SK28 cells. These currents are mediated by a diversity of ion channels such as inward rectifying  $K^+$  channels,  $Ca^{2+}$ -activated  $K^+$  channels,  $Ca^{2+}$ ,  $Cl^-$ , and  $Na^+$  channels (Allen et al., 1997). However, in only one of these cell lines (C8146) an outwardly rectifying  $K^+$  channel was expressed. In contrast, we found in all three tested melanoma cell lines (IGR1, IGR39, and IPC298) outwardly rectifying  $K^+$  channels, albeit with variable expression level. The channels in IGR1 have previously been functionally characterized on the single-channel level by Nilius, Böhm & Wohlrab (1990) concluding at that time that this channel is a delayed rectifier, which is modulated by

$\beta$ -adrenergic interventions. Here we demonstrated that IGR1 and IPC298 cells express human *ether à go-go* channels, whereas IGR39 cells express typical delayed-rectifier channels. Using RT-PCR analysis we could amplify a DNA fragment identical to h-eag1. Thus, it is interesting to note that various melanoma cell lines are by no means homogeneous in terms of their expressed ion channels. The variable expression pattern of ion channels in melanoma cells may be attributed to their neuronal crest lineage. In addition, transformation of melanocytes into variable cell types during tumor generation may be a possible explanation.

Judged from the whole-cell current amplitudes in IGR1 cells, small- and intermediate conductance  $Ca^{2+}$ -activated  $K^+$  channels are abundantly expressed in these cells. Using RT-PCR methods, we could identify hSK1, hSK2, and hIK channels in IGR1 cells.  $Ca^{2+}$ -activated  $K^+$  channels were also described in other melanoma cell lines. They were separated in charybdotoxin-sensitive (SK28, C8146) and apamin-sensitive (C8161) (Allen, Lepple-Wienhues & Cahalan, 1997) channels. The channels in IGR1 are insensitive for apamin, a property shared by recombinant rSK1 channels (Ishi, Maylic & Adelman, 1997a). rSK2 channels, however, should be very sensitive to apamin (Köhler et al., 1996; Ishi et al., 1997a). rSK2 channels were shown to be sensitive to  $\alpha$ -tubocurarine, while hSK1 channels are less sensitive (Ishi et al., 1997a). In addition, recombinant hIK1 channels expressed in *Xenopus* oocytes were shown to be sensitive to both ChTx ( $IC_{50} \approx 2.5$  nM) and clotrimazole ( $IC_{50} \approx 25$  nM) (Ishi et al., 1997b). Somewhat different results were obtained for the identical channel hKCa4, expressed in HEK293 cells (ChTx:  $10$  nM; clotrimazole:

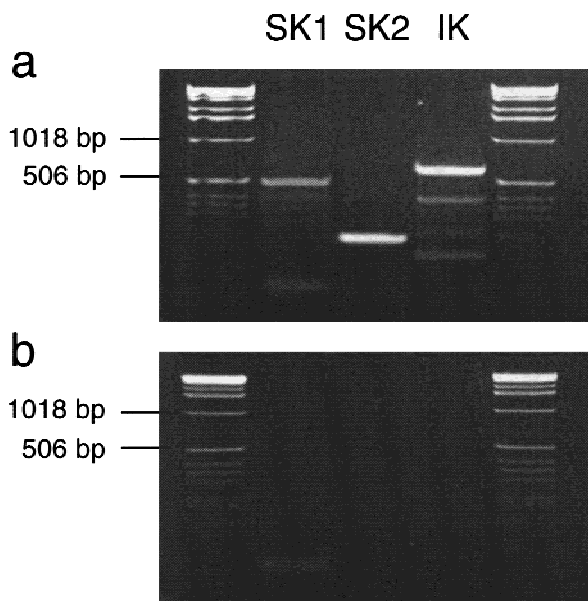


**Fig. 6.** (a) Expression of hSK1, hSK2, and hIK in IGR1 cells. RT-PCR products from IGR1 mRNA generated with gene-specific primers were analyzed on a 2% agarose gel. The strongest bands in each lane show the expected fragment sizes of 495 bp (hSK1), 203 bp (hSK2), and 599 bp (hIK) and the identity of the products was confirmed by DNA sequencing. (b) Control reaction with the same primers as in a, but replacing the 50°C reverse transcription by a 5-min step at 95°C in order to inactivate reverse transcriptase.

387 nM; Logsdon et al., 1997). Thus, the partial block of  $K(Ca^{2+})$  channels in IGR1 cells by ChTx and clotrimazole is consistent with the functional expression of hIK channels in these cells. Given the expression of various SK and IK sequences (Fig. 6), the possibility that some of these subunits form heterooligomeric channels (Ishi et al., 1997a), and the discrepancy of results obtained from cloned channels, it is not straightforward to determine which type of  $K(Ca^{2+})$  channel makes the major contribution to calcium-activated currents in IGR1 cells. Based on the lack of apamin and *d*-tubocurarine block, however, it seems unlikely that homomeric hSK2 channels are expressed abundantly. Interestingly, in electrophysiological measurements we did not detect an appreciable expression of inwardly rectifying channels, suggesting that the establishment of the cell resting potential relies on hSK1, hIK, and maybe h-eag1 channels.

Both molecularly identified  $K^{+}$  channel types depend on intracellular  $Ca^{2+}$ . h-eag1 channels in melanoma cells are half-maximally blocked by less than 100 nM free cytosolic  $Ca^{2+}$ . In this respect these channels are identical to the recombinant versions (Bijlenga et al., 1998) or those expressed in neuroblastoma cells (Meyer & Heinemann, 1998). hSK/hIK channels, however, are activated at  $Ca^{2+}$  concentrations above 100 nM and full activation is obtained at about 1  $\mu$ M. Thus, by the simultaneous expression of h-eag1 and small- and inter-

mediate conductance  $K(Ca^{2+})$  channels, some melanoma cell types will exhibit a minimum in  $K^{+}$  conductances as a function of intracellular  $Ca^{2+}$  at around 200 nM.

In nonexcitable cells, like melanoma cells, the most obvious function of  $K^{+}$  channels is the control of the resting potential. IGR1 cells with low intracellular  $Ca^{2+}$ , and therefore active h-eag1 but inactive  $K(Ca^{2+})$  channels, reveal a resting potential in the range of  $-20$  to  $-40$  mV. Very similar values of approximately  $-32$  mV were reported for myoblasts expressing h-eag1 channels (Bernheim et al., 1996; Occhiodoro et al., 1998). Thus, h-eag1 channels may just limit the resting potential to these values, which match with their activation threshold (see Fig. 1a and b). Activation of  $K(Ca^{2+})$  channels in IGR1 resulted in a hyperpolarization of the membrane to  $-70$  to  $-80$  mV.

These are important functional features since there are indications that changes of the membrane potential play a role in cell cycle progression. In some cells (e.g., Chinese hamster V79, Neuro-2A neuroblastoma, MCF-7) a large hyperpolarization is reported between early G1 and transition to S phase. In addition, depolarization of the membrane by increasing the extracellular  $K^{+}$  concentration inhibited cell proliferation (Wonderlin & Strobl, 1996). Furthermore, studies with embryonic rat cortical cells revealed two cell populations with distinct resting potentials at about  $-40$  and  $-70$  mV. Depolarized cells were proliferative and their resting potentials were sensitive to extracellular  $Ca^{2+}$ , whereas hyperpolarized cells were postmitotic and expressed  $Ca^{2+}/Ba^{2+}$ -sensitive and  $Ca^{2+}$ -dependent  $K^{+}$  channels (Maric et al., 1998).

Since h-eag1 and hSK/hIK of human melanoma cells are capable of influencing the resting potential, they may be important for proliferation or differentiation processes. Both channel types are regulated by intracellular  $Ca^{2+}$ , the most common second messenger involved in many different cellular processes such as, i.e., muscle contraction, neurotransmitter release, or cell proliferation. For tumor cells, the influence on proliferation is of special interest and it is known that an increase of cytosolic  $Ca^{2+}$  is required at two stages of the cell-cycle, the G0/G1 and the G1/S transition (Wonderlin & Strobl, 1996). Therefore,  $Ca^{2+}$  signals are potential candidates for regulating the resting potential generated by h-eag1 and hSK/hIK channels.

Cell proliferation may be influenced by  $K^{+}$  channels, but, on the other hand, the cell-cycle can regulate the expression of  $K^{+}$  channels. Especially, the voltage-gated eag channel seems to be strongly influenced by cell development. Maturation of *Xenopus* oocytes induced a reduction of the current mediated by cloned r-eag channels expressed in these cells (Brüggemann, Stühmer & Pardo, 1997). In addition, the expression of endogenous h-eag channels in neuroblastoma cells is downregulated after induction of differentiation with retinoic acid (Meyer



& Heinemann, 1998). Moreover, in myoblasts the expression of h-eag1 is coupled to early steps of differentiation and declines at the end of differentiation, which is in these cells marked by cell fusion (Occhiodoro et al., 1998). In all three studies, eag channels could not be detected in differentiated cells. However, eag channels were detected in cells arrested in the G<sub>2</sub>-phase (Brüggemann et al., 1997), in proliferating cells (Meyer & Heinemann, 1998), or in cells at the onset of differentiation (Occhiodoro et al., 1998). These findings suggest a function of eag channels in proliferation of IGR1 and IPC298 melanoma cells. Upon delineation of the molecular interplay between expression of h-eag1 and hSK/hIK channels, resting potential, intracellular Ca<sup>2+</sup>, and proliferative potential, h-eag1 or hSK/hIK channels may become molecular targets with diagnostic or even therapeutic relevance.

This work was supported by the Max-Planck Society and the DFG (SFB 197, TP A8 and A14). We are grateful to the technical assistance by S. Arend and A. Rossner.

## References

- Allen, D.H., Lepple-Wienhues, A., Cahalan, M.D. 1997. Ion channel phenotype of melanoma cell lines. *J. Membrane Biol.* **155**:27–34
- Bernheim, L., Liu, J.-H., Hamann, M., Haenggeli, C.A., Fischer-Lougheed, J., Bader, C.R. 1996. Contribution of a non-inactivating potassium current to the resting membrane potential of fusion-competent human myoblasts. *J. Physiol.* **493**:129–141
- Bijlenga, P., Occhiodoro, T., Liu, J.H., Bader, C.R., Bernheim, L., Fischer-Logheed, J. 1998. An *ether-à-go-go* K<sup>+</sup> current, *I*<sub>h-eag</sub>, contributes to the hyperpolarization of human fusion-competent myoblasts. *J. Physiol.* **512**:317–323
- Brüggemann, A., Stühmer, W., Pardo, L.A. 1997. Mitosis-promoting factor-mediated suppression of a cloned delayed rectifier potassium channel expressed in *Xenopus* oocytes. *Proc. Natl. Acad. Sci. USA* **94**:537–542
- Frings, S., Brüll, N., Dzeja, C., Angele, A., Hagen, V., Kaupp, U.B., Baumann, A. 1998. Characterization of *ether-à-go-go* channels present in photoreceptors reveals similarity to *I*<sub>KX</sub>, a K<sup>+</sup> current in rod inner segments. *J. Gen. Physiol.* **111**:583–599
- Ishi, T.M., Maylie, J., Adelman, J.P., 1997a. Determinants of apamin and d-tubocurarine block in SK potassium channels. *J. Biol. Chem.* **272**:23195–23200
- Ishi, T.M., Silvia, C., Hirschberg, B., Bond, C.T., Adelman, J.P., Maylie, J. 1997b. A human intermediate conductance calcium-activated potassium channel. *PNAS USA* **94**:11651–11656
- Joiner, W.J., Wang, L.-Y., Tang, M.D., Kaczmarek, L.K. 1997. hSK4, a member of a novel subfamily of calcium-activated potassium channels. *PNAS USA* **94**:11013–11018
- Köhler, M., Hirschberg, B., Bond, C.T., Kinzie, J.M., Marrion, N.V., Maylie, J., Adelman, J.P. 1996. Small-conductance, calcium-activated potassium channels from mammalian brain. *Science* **273**:1709–1714
- Lepple-Wienhues, A., Berweck, S., Böhmig, M., Leo, C.P., Meyling, B., Garbe, C., Wiederholt, M. 1996. K<sup>+</sup> channels and the intracellular calcium signal in human melanoma cell proliferation. *J. Membrane Biol.* **151**:149–157
- Logsdon, N.J., Kang, J., Togo, J.A., Christian, E.P., Aiyar, J. 1997. A novel gene, *hKCa4*, encodes the calcium-activated potassium channel in T lymphocytes. *J. Biol. Chem.* **272**:32723–32726
- Ludwig, J., Terlau, H., Wunder, F., Brüggemann, A., Pardo, L.A., Marquardt, A., Stühmer, W., Pongs, O. 1994. Functional expression of rat homologue of the voltage gated *ether à go-go* potassium channel reveals differences in selectivity and activation kinetics between *Drosophila* channel and its mammalian counterpart. *EMBO J.* **13**:4451–4458
- Maric, D., Maric, I., Smith, S.V., Serafini, R., Hu, Q., Barker, J.L. 1998. Potentiometric study of resting potential, contributing K<sup>+</sup> channels and the onset of Na<sup>+</sup> channel excitability in embryonic rat cortical cells. *Eur. J. Neurosci.* **10**:2532–2546
- Meyer, R., Heinemann, S.H. 1998. Characterization of an eag-like potassium channel in human neuroblastoma cells. *J. Physiol.* **508**:49–56
- Neher, E. 1995. The use of Fura-2 for estimating Ca<sup>2+</sup> buffers and Ca<sup>2+</sup> fluxes. *Neuropharmacol.* **34**:1423–1442
- Nilius, B., Böhm, T., Wohlrab, W. 1990. Properties of a potassium-selective ion channel in human melanoma cells. *Pfluegers Arch.* **417**:269–277
- Nilius, B., Schwarz, G., Droogmans, G. 1993. Control of intracellular calcium by membrane potential in human melanoma cells. *Am. J. Physiol.* **265**:1501–1510
- Nilius, B., Wohlrab, W. 1992. Potassium channels and regulation of proliferation of human melanoma cells. *J. Physiol.* **445**:537–548
- Occhiodoro, T., Bernheim, L., Liu, J.-H., Bijlenga, P., Sinnreich, M., Bader, C.R., Fischer-Lougheed, J. 1998. Cloning of a human *ether à go-go* potassium channel expressed in myoblasts at the onset of fusion. *FEBS Lett.* **434**:177–182
- Peña, T.L., Rane, S.G. 1997. The small conductance calcium-activated potassium channel regulates ion channel expression in C3H10T1/2 cells ectopically expressing the muscle regulatory factor MRF4\*. *J. Biol. Chem.* **272**:21909–21916
- Schönherr, R., Hehl, S., Terlau, H., Baumann, A., Heinemann, S.H. 1999. Individual subunits contribute independently to slow gating of bovine EAG potassium channels. *J. Biol. Chem.* **274**:5362–5369
- Stansfeld, C.E., Pöper, J., Ludwig, J., Weseloh, R.M., Marsh, S.J., Brown, D.A., Pongs, O. 1996. Elevation of intracellular calcium by muscarinic receptor activation induces a block of voltage-activated rat *ether à go-go* channels in a stably transfected cell line. *Proc. Natl. Acad. Sci. USA* **93**:9910–9914
- Terlau, H., Ludwig, J., Steffan, R., Pongs, O., Stühmer, W., Heinemann, S.H. 1996. Extracellular Mg<sup>2+</sup> regulates activation of rat eag potassium channel. *Pfluegers Arch.* **432**:301–321
- Vergara, C., Latorre, R., Marrion, N.V., Adelman, J.P. 1998. Calcium-activated potassium channels. *Curr. Op. Neurobiol.* **8**:321–329
- Wonderlin, W.F., Strobl, J.S. 1996. Potassium channels, proliferation and G1 progression. *J. Membrane Biol.* **154**:91–107